arXiv:1112.3830v1 [quant-ph] 16 Dec 2011

Determining final probabilities directly from the initial state

A. S. Sanz and S. Miret-Artés
Instituto de Física Fundamental - CSIC, Serrano 123, 28006 Madrid, Spain.
(Dated: December 19, 2011)

In quantum scattering problems it is not possible to relate unambiguously a particular feature of the final outcome with some specific section of the initial state. As it is shown here, this drawback can be overcome by conveniently combining the divergence or Gauss-Ostrogradsky theorem with Bohmian mechanics. This renders a general approach which enables such a connection and allows us to determine the value of final partial or restricted probabilities directly from the corresponding localized section of the initial state. As an illustration, this approach is applied to two prototypical scattering phenomena: tunneling and grating diffraction.

PACS numbers: 03.65.-w, 03.65.Ca, 03.65.Nk, 03.75.-b, 03.65.Xp

I. INTRODUCTION

Unlike classical mechanics, quantum mechanics poses an important problem when dealing with scattering problems: although desirable, it is not possible to establish an unambiguous relationship between a particular feature of the final outcome and some specific part of the initial state. Within standard quantum mechanics we find robust theoretical frameworks to tackle scattering problems [1] as well as efficient numerical algorithms [2] when the former are not enough. However, they forbid the possibility to only compute the probabilities related to such features (i.e., partial or restricted probabilities) from a certain set of initial conditions, as it can be done in (statistical) classical mechanics by means of an appropriate sampling.

In this work we propose a way to attack this kind of problems, which combines the divergence or Gauss-Ostrogradsky theorem with Bohmian mechanics [3, 4]. As it is well known, in standard quantum mechanics the divergence theorem allows to establish a connection between the variation of the probability density ρ confined within a certain (configuration space) region of volume V with its flux across the boundary surface S of such a region, which is accounted for by the probability current density $\mathbf{J}$. Formally, this is expressed in terms of the well-known continuity equation

$$\frac{\partial \rho}{\partial t} + \nabla \mathbf{J} = 0. \tag{1}$$

On the other hand, the possibility to define the analog of a classical trajectory in Bohmian mechanics, namely a Bohmian or quantum trajectory, is also of much help, for it allows us to associate (1) with ensemble-like descriptions. Thus, consider we want to compute the probability inside some subregion of the configuration space, Σ, that encloses one particular scattering feature. For example, this region may represent the boundaries embracing a particular diffraction peak in scattering problems or the transmission probability in tunneling problems. Usually, in a typical time-dependent quantum-mechanical simulation [2], one lets the process to propagate in time until a certain final configuration (state) is reached. In general, it is common to choose asymptotic, stationary configurations, which are closer to analytical time-independent derivations [1], but this requirement is not always necessary. Then, one computes the partial fraction of the total probability that has gone into Σ, namely the *restricted probability* [5–7], which is given by

$$\mathcal{P}_\Sigma(\infty) \equiv \lim_{t\to\infty} \mathcal{P}_\Sigma(t) = \lim_{t\to\infty} \int_\Sigma \rho(\mathbf{r},t) d\mathbf{r}. \tag{2}$$

This quantity is precisely directly related to the problem posed above.

As it is shown that, making use of Bohmian mechanics, if the set of quantum trajectories lying down on the boundary of Σ at t is known, restricted probabilities like (2) can be directly evaluated from the initial state at t_0. In virtue of the causal (Bohmian) connection between two configuration space points at two different times, the final positions of the trajectories forming the boundaries of Σ are unambiguously associated with a certain set of initial conditions that constitute the boundaries of a region Σ_0 at t_0. This implies that any trajectory starting inside Σ_0 will end up inside Σ at t. Therefore, the restricted probability enclosed by the set of trajectories forming the boundaries of Σ_0 will remain constant along time, allowing us to compute $\mathcal{P}_\Sigma(t)$ directly from the initial state. Indeed, it is also possible to obtain a one-to-one relationship between a specific part of the initial state and a particular feature of the outgoing state that we might be interested in; at each time, one has full knowledge of where the probability confined within a particular Σ_0 goes. It is worth noticing that, within the standard formulation of quantum mechanics, there is no way to determine this key information, which can be used in a rather practical way to conduct dynamical analyses of isolate scattering features in matter wave experiments [8] or quantum control scenarios [9], for example. The generality of this result is proven for two prototypical processes found in scattering problems: tunneling and grating diffraction.

This work is organized as follows. In Sec. II, the general theoretical framework that justifies our approach is introduced. In Sec. III, some applications will be considered. First, as a simple analytical illustration of the assertions discussed in Sec. II, the case of a Gaussian slit diffraction will be exposed. Then, some numerical simulations for tunneling and grating diffraction will be presented. Finally, the main conclusions extracted from this work are summarized in Sec. IV.

II. THEORETICAL FRAMEWORK

Let $P(t)$ be the probability describing a certain property of a quantum system of mass m inside a volume V of its associated configuration space at a given time t, i.e.,

$$P(t) = \int_V \rho(\mathbf{r}, t) d\mathbf{r}, \tag{3}$$

where $\rho(\mathbf{r}, t) = |\Psi(\mathbf{r}, t)|^2$ and the system wave function Ψ satisfy the corresponding Schrödinger equation. The variation with time of $P(t)$ within V is given by

$$\frac{dP(t)}{dt} = \int_V \frac{\partial \rho}{\partial t}\, d\mathbf{r}, \tag{4}$$

which can also be expressed as

$$\frac{dP(t)}{dt} = -\int_V (\nabla \cdot \mathbf{J})\, d\mathbf{r} = -\int_S \mathbf{J} \cdot d\mathbf{S}, \tag{5}$$

according to the continuity equation (1), where $d\mathbf{S}$ in the second equality is a vector normal to a surface element dS on S and pointing outwards. From the application of the divergence theorem in this second equality, it follows that the losses or gains of $P(t)$ inside V are described by the probability flow through S, which is quantified by the quantum current density $\mathbf{J}$. Physically, this is a very clear and elegant result to describe the conservation of probability. However, from a more practical point of view, it presents a serious drawback. In order to understand it, consider a classical system, for which the same conservation equation holds (with ρ describing a density distribution). Let Σ_1 and Σ_2 be two regions with surfaces S_1 and S_2, respectively. Both regions are assumed to be embedded in the system phase space at times t_1 and t_2, respectively, with $t_2 > t_1$. Moreover, each point on S_2 is causally connected with one point on S_1 by means of a (classical) trajectory (solution of Hamilton's equations of motion). Then, any swarm of trajectories confined within Σ_1 at t_1 will end up inside Σ_2 at t_2, this being the trait of a conservative Liouvillian dynamics or, in other words, of the conservation equation for a classical system. In standard quantum mechanics, on the contrary, there is no way at all to define such a mapping transformation, for there is no rule that allows us to connect the two regions Σ_1 and Σ_2. Even if one defines tubes along which the probability flows, there is nothing preventing it to scape from or to enter into such tubes, in general, because it is not possible to establish a causal connection that describes the generation of these tubes when Σ_1 evolves in time to Σ_2.

In order to establish such a connection one has to consider Bohmian mechanics, where the flow of quantum probabilities can be monitored by means of quantum trajectories (this flow, indeed, will define the probability tubes that we need). Bohmian or quantum trajectories are solutions of the equation of motion

$$\dot{\mathbf{r}} = \frac{\nabla S}{m} = \frac{\mathbf{J}}{\rho}. \tag{6}$$

This equation is identical to the classical Jacobi law of motion [10], although here S refers to the phase of the wave function when it is written in polar form, i.e., $\Psi(\mathbf{r}, t) = \rho^{1/2}(\mathbf{r}, t) e^{iS(\mathbf{r},t)/\hbar}$, instead of to a classical action. Nonetheless, it can also be defined if a local velocity field is introduced according to the relation $\mathbf{J} = \rho\mathbf{v}$ [second equality in (6)], which describes how the quantum probability density is transported through the configuration space in the form of the quantum probability current density by means of a drift (local) velocity field $\mathbf{v}$. Thus, consider Σ_0 is a certain region of the system configuration space covered by swarm of initial conditions distributed randomly according to $\rho_0(\mathbf{r}) = |\Psi_0(\mathbf{r})|^2$, as it is also commonly found when dealing with statistical classical mechanics (i.e., just like in any standard classical Monte-Carlo sampling). The corresponding trajectories will then reach another region Σ at a time t causally connected with Σ_0, such that the positions of the trajectories follow a random distribution according to $\rho(\mathbf{r}, t) = |\Psi(\mathbf{r}, t)|^2$. Because of the non-crossing property of quantum fluxes (or, equivalently, quantum trajectories) [11], similarly to classical mechanics no (quantum) trajectories will scape from or enter into the probability tube defined by the evolution of Σ_0 along time. Therefore, the probability inside, proportional to the number of trajectories confined within the boundaries of Σ, will remain constant along time. From now on, those trajectories starting just on points belonging to the surface of Σ_0 will be called *separatrix trajectories*, for they separate the probability inside the tube from the rest in virtue of the non-crossing flux property.

The previous argument can be reverted, this implying that given the end points of the separatrix trajectories associated with Σ, one can obtain the boundaries of Σ_0 and, therefore, determine the probability inside Σ without carrying out the full simulation, but only knowing the associated section from the initial wave function (i.e., the portion of the initial wave function lying down within the boundaries of Σ_0). In order to proof this statement, consider for simplicity (but without loss of generality) a one-dimensional problem, where Σ is defined as the region delimited by two given points x_1^∞ and x_2^∞ asymptotically. By "asymptotic" it is meant the Fraunhofer domain [12], where the probability density remains stationary, i.e., its relative shape does not change with time, but remains re-scalable. As shown in Ref. [13], these points can be associated with the positions of two boundary (separatrix) quantum trajectories (which, within the Fraunhofer regime, are also re-scalable, following the laws of uniform motion). Because these trajectories can be propagated backwards in time according to Eq. (6), Eq. (2) can be reexpressed as

$$\begin{aligned}\mathcal{P}_\Sigma(\infty) &= \int_{x_1^\infty}^{x_2^\infty} \rho(x^\infty) dx^\infty \\ &= \lim_{t\to\infty} \int_{x_1(t)}^{x_2(t)} \rho[x(t)]dx(t) = \lim_{t\to\infty} \mathcal{P}_\Sigma(t), \quad (7)\end{aligned}$$

where $\rho(x^\infty)dx^\infty$ is the probability to find the system confined between x^∞ and $x^\infty + dx^\infty$; $\rho[x(t)]dx(t)$ is the probability to find the system confined between $x(t)$ and $x(t) + dx(t)$; and the time-dependence denotes a causal connection, e.g., $x^\infty = \lim_{t\to\infty} x(t)$. The time-dependence of the probability density is purposely specified as $\rho[x(t)]$ instead of $\rho(x,t)$ in order to stress the fact that, at any time t, it is evaluated along quantum trajectories rather than on arbitrary points of the configuration space (this also emphasizes the fact that quantum trajectories are paths along which probability flows in configuration space).

Since Bohmian trajectories can be traced back in time, from t to their initial condition, the limit in the second equality in Eq. (7) can be removed, so that $\mathcal{P}_\Sigma(\infty)$ can be recast as an integral over the system initial state,

$$\mathcal{P}_\Sigma(\infty) = \int_{x_1(0)}^{x_2(0)} \rho[x(0)]dx(0) = \mathcal{P}_\Sigma(0), \quad (8)$$

which is the same to say that it can be obtained just from a sampling over initial conditions (for the quantum trajectories). This is a result of *general* validity, which just states that the probability in a certain region of the configuration space can be transported to another one unambiguously, i.e., following causally (by means of Bohmian mechanics) the evolution of the boundaries of such an initial region. As it can be inferred, this result goes beyond standard quantum mechanics, for although it is possible to define tubes along which the probability flows and surfaces traversed by such flows, as mentioned above there is no rule accounting for the evolution of probability tubes, thus avoiding to establish any univocal relationship between regions Σ defined at different times. As a consequence, we find that, in principle, the knowledge of both the initial state and some particular initial conditions of interest, $x_1(0)$ and $x_2(0)$, allows us to determine quantities like transmission probabilities or diffraction intensities (or an estimate of them without performing the whole dynamical calculation provided we have a fair guess [13]).

Furthermore, it is also worth stressing the strong connection between Eq. (8) and the so-called Born rule [14]. Indeed, the combination of the quantum continuity equation and Bohmian mechanics makes Eq. (8) to incorporate implicitly a kind of time-dependent Born rule. In this regard, it is interesting to note that, instead of the two limiting times $t \to \infty$ and $t = 0$, one can also consider two arbitrary times, t and t' (we will assume $t' > t$). Then, from Eq. (8), it follows that

$$\int_{x_1(t')}^{x_2(t')} \rho[x(t')]dx(t') = \int_{x_1(t)}^{x_2(t)} \rho[x(t)]dx(t). \quad (9)$$

On the other hand, because of the causal connection between $x(t)$ and $x(t')$ in Bohmian mechanics, one can also define a Jacobian

$$\mathcal{J}[x(t)] = \frac{\partial x(t')}{\partial x(t)}, \quad (10)$$

which describes the mapping transformation in configuration space from $x(t)$ at a time t to $x(t')$ at a time t', as it is well known from classical mechanics [15, 16]. Taking thus into account the equality (9) and the connection between $dx(t)$ and $dx(t')$ enabled by the Jacobian,

$$dx(t') = |\mathcal{J}[x(t)]|\, dx(t), \quad (11)$$

one finds that the probability density evaluated along a Bohmian trajectory at a given time t' is related through the inverse Jacobian transformation with its value at an earlier time t, i.e.,

$$\rho[x(t')] = |\mathcal{J}[x(t')]|\, \rho[x(t)], \quad (12)$$

with $|\mathcal{J}[x(t')]| = |\mathcal{J}[x(t)]|^{-1}$. In other words, this result states that Born's rule preserves along time whenever the evolution of the probability $\rho[x(t)]$ is monitored between two Bohmian trajectories $x(t)$ and $x'(t) = x(t) + dx(t)$, i.e.,

$$\rho[x(t')]dx(t') = \rho[x(t)]dx(t), \quad (13)$$

as in classical mechanics [15, 16].

III. APPLICATIONS

A. Gaussian slit diffraction

The free evolution of a quantum system of mass m after undergoing diffraction by a Gaussian slit constitutes a simple example to illustrate the assertions from Sec. II. Thus, consider the wave function describing the system just after the diffraction process is given by

$$\Psi_0(x) = A_0\, e^{-(x-x_0)^2/4\sigma_0^2 + ip_0(x-x_0)/\hbar}, \quad (14)$$

where $A_0 = (2\pi\sigma_0^2)^{-1/4}$ is the normalization constant, x_0 and p_0 are respectively the (initial) position and momentum of its centroid [i.e., $\langle \hat{x} \rangle = x_0$ and $\langle \hat{p} \rangle = p_0$], and σ_0 its initial spreading. The time-evolution of this wave packet is described by

$$\Psi(x,t) = A_t\, e^{-(x-x_{\rm cl})^2/4\tilde{\sigma}_t\sigma_0 + ip_{\rm cl}(x-x_{\rm cl})/\hbar + iE_{\rm cl}t/\hbar}, \quad (15)$$

with $A_t = (2\pi\tilde{\sigma}_t^2)^{-1/4}$, $\tilde{\sigma}_t = \sigma_0(1 + i\hbar t/2m\sigma_0^2)$ and $E_{\rm cl} = p_0^2/2m$. The shape of this wave packet does not change with time, but only its width undergoes a monotonic increase, as

$$\sigma_t = |\tilde{\sigma}_t| = \sigma_0 \sqrt{1 + \left(\frac{\hbar t}{2m\sigma_0^2} \right)^2} , \tag{16}$$

while its centroid evolves according to a classical uniform motion, i.e., $x_{\rm cl} = x_0 + v_0 t$ and $p_{\rm cl} = p_0$. The associated probability density thus looks the same at any time,

$$\rho(x,t) = \frac{1}{\sqrt{2\pi\sigma_t^2}} \, e^{-(x-x_{\rm cl})^2/2\sigma_t^2} . \tag{17}$$

The Bohmian trajectories associated with (15) are readily obtained after integrating the corresponding equation of motion, to yield

$$x(t) = x_{\rm cl} + \frac{\sigma_t}{\sigma_0} \left[x(0) - x_0 \right] . \tag{18}$$

From this expression, the associated Jacobian reads as

$$\mathcal{J}[x(0)] = \frac{\partial x(t)}{\partial x(0)} = \frac{\sigma_t}{\sigma_0} , \tag{19}$$

which leads to

$$\begin{aligned} dx(t) &= |\mathcal{J}[x(0)]| \, dx(0), & (20) \\ \rho(x(t)) &= |\mathcal{J}[x(t)]| \, \rho(x(0)), & (21) \end{aligned}$$

with $|\mathcal{J}[x(t)]| = |\mathcal{J}[x(0)]|^{-1} = \sigma_0/\sigma_t$ ruling the backwards mapping transformation, from t to $t_0 = 0$. If these expressions are now substituted into Eq. (7), we readily find Eq. (8) or, equivalently, Eq. (13).

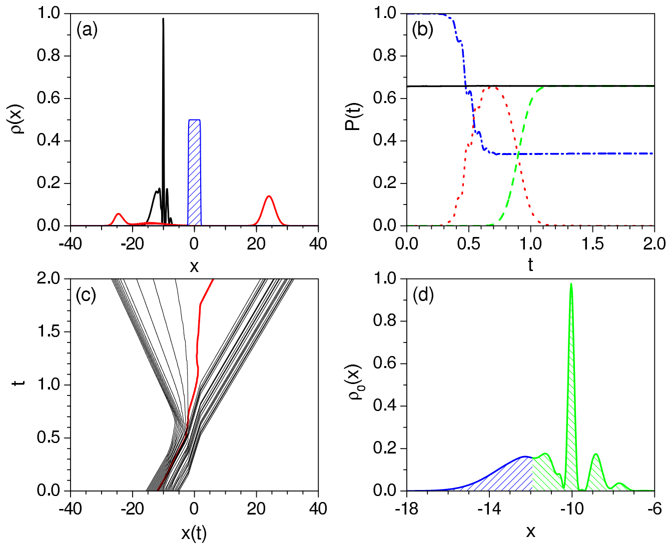

FIG. 1: (a) Initial (black line) and asymptotic, final (red line) probability densities representing the tunneling of a wave packet with an arbitrary shape through a quasi-squared barrier (blue shadowed region). (b) Time-dependence of the different restricted probabilities: transmission (green dashed line), reflection (blue dash-dotted line) and intra-barrier resonance (red dotted line) probabilities. The transmission probabilities directly computed from the initial state accounting only the associated quantum trajectories is displayed with black solid line. (c) Quantum trajectories illustrating the tunneling dynamics. The separatrix trajectory is denoted with the red thicker line. (d) Separation in two sections of the initial probability density according to the separatrix trajectory. Only the green shadowed region will contribute to the transmittance, while the blue shadowed section will be scattered backwards, contributing to the reflectance.

B. Tunneling

Usually, within the energy domain, the calculation of properties related to tunneling through barriers (transmittances, reflectances or intra-barrier resonances) is carried out by means of stationary wave approaches, where the system wave function and its first derivative have to satisfy some matching and/or boundary conditions at the barrier edges [1, 17]. The approach presented above, on the contrary, enables the calculation of such properties in a more straightforward fashion, directly from the initial state once the separatrix trajectories are determined [13]. Thus, we have considered the scattering with a barrier of a wave packet consisting of a coherent sum of three Gaussian wave packets,

$$\Psi_0(x) = \sum_{i=1}^{3} c_i \psi_i(x), \tag{22}$$

with each ψ_i having the same form as (14). In particular, in the example shown here the parameters chosen are: $(c_1, c_2, c_3) = (1.0, 0.75, 0.5)$, $(x_{0,1}, x_{0,2}, x_{0,3}) = (-10, -12, -9)$, $(p_{0,1}, p_{0,2}, p_{0,3}) = (10, 20, 15)$, $(\sigma_{0,1}, \sigma_{0,2}, \sigma_{0,3}) = (0.2, 1.6, 0.8)$, and $m = \hbar = 1$; after introducing these values, the wave function Ψ_0 was properly renormalized before starting the simulation. Regarding the barrier, it was a quasi-squared barrier consisting of a sum of two hyperbolic tangents,

$$V(x) = \frac{V_0}{2} \left\{ \tanh\left[\alpha(x - x_-)\right] - \tanh\left[\alpha(x - x_+)\right] \right\} , \tag{23}$$

with $V_0 = 150$, $\alpha = 10$, and $x_\pm = \pm 2$. As shown below, this example will allow us to illustrate the generality of Eq. (8) with respect to the election of the initial state (initial condition) or the type of barrier (problem).

The initial and final probability densities are displayed in Fig. 1(a) (with black and red solid lines, respectively); the barrier has also been plotted (blue shadowed region). Regarding the final state, the system has been let to evolve until the probability in the region covered by the barrier (intra-barrier resonance) was negligible, this being considered the asymptotic time. This can be better appreciated in Fig. 2(b), where the transmission (green dashed line), reflection (blue dash-dotted line) and intra-barrier resonance (red dotted line) probabilities are monitored along time. These three restricted probabilities are computed assuming the corresponding regions are as follows: $\Sigma_{\rm trans}$ is the region beyond the right edge of the barrier, $\Sigma_{\rm res}$ is the region bound between the two edges of the barrier, and $\Sigma_{\rm refl}$ is the region to the left edge of the barrier. As it can be seen, after $t \approx 1.15$, $\mathcal{P}_{\Sigma_{\rm res}} \approx 0$ and $\mathcal{P}_{\Sigma_{\rm trans}}$ reaches its maximum, asymptotic value; $\mathcal{P}_{\Sigma_{\rm refl}}$, on the contrary, reaches its minimum earlier, at $t \approx 0.75$.

Taken that into account, we decide to split the asymptotic state between transmission and reflection, with the region Σ_0 being being associated with the former. Initially, the upper boundary of this region can be any trajectory to the right border of the initial probability density, such that the associated probability density is negligible, i.e., $\rho(x_0) \approx 0$. For the lower boundary, a search has to be done [13], so that it is ensured that the chosen trajectory is the last one in passing the barrier with a negligible value of the associated probability density. This can be determined by means of a series of sampling runs or just fixing the asymptotic value of the trajectory and running backwards the dynamics until $t = 0$. In Fig. 1(c), a sampling set of quantum trajectories is shown. These trajectories have been evenly distributed along the whole extension covered by the initial probability density to better illustrate the dynamics. In this case, the red thicker line denotes the separatrix trajectory which separates the initial swarm into two groups: those that will surmount the barrier and those that will bounce backwards. This means that, in this case, the region Σ (the time-evolved of Σ_0) is specified only by one separatrix trajectory. When this is translated into the initial probability density, we find which part of it will contribute to transmission and which one not [see Fig. 1(d)]. Thus, if we compute the integral over the green shadowed region displayed in Fig. 1(d) and follow it along time taking into account where the separatrix trajectory is at each time, we obtain the black solid line plotted in Fig. 1(c). This curve presents a constant value at any time, which coincides with the asymptotic value of the transmission probability, thus proving our assertion that final probabilities can be computed directly from the initial state and, as it will be shown with the next example, this can only be done by means of Bohmian trajectories.

C. Grating diffraction

Quantum trajectories have been used in the past to determine the boundaries in the initial probability density that separate contributions associated with different specific features in both [12] and slit diffraction [18]. By means of the approach introduced in Sec. II, one can take these studies further away, to a more quantitative and applied level. Thus, consider one would like to determine an observable in any of these scattering problems, such as the so-called *peak-area intensity*, for example, which is the integral of the probability density covered by a particular diffraction peak. Physically, this quantity provides us with the relative amount of diffracted particles lying within the width covered by the corresponding diffraction peak. According to the tools developed so far, in particular Eq. (17), this quantity can be obtained directly from the initial wave function once the two trajectories delimiting the corresponding peak are determined, just as in the example of tunneling described above. To illustrate this problem, for simplicity (but without loss of generality), we consider the case of multiple-slit diffraction, which is isomorphic to that of scattering by a periodic reflection grating [18]. Thus, a five-slit array of Gaussian slits is assumed, so that the outgoing wave can be represented by a coherent superposition of five identical Gaussian wave packets, like (14),

$$\Psi_0(x) = \sum_{i=1}^{5} \psi_{(}x), \qquad (24)$$

where $x_0^{(i)} = -4 + 2(i-1)$, $p_0^{(i)} = p_0 = 0$ (zero transverse momentum), $\sigma_0^{(i)} = \sigma_0 = 0.2$, and $m = \hbar = 1$; as before, after introducing these values, the wave function Ψ_0 was properly normalized before conducting the simulation. Note that we have implicitly assumed that the propagation along the direction perpendicular to the grating is too large compared to the evolution along the transversal one, this enabling this simplified one-dimensional treatment, where we only focus on the diffractive and interference effects that take place along the transversal direction. Furthermore, now the wave packet will not be allowed to evolve asymptotically, until all the minima are well defined (i.e., when the probability density at such values vanishes), but only until they can be well resolved (i.e., when the distance betweeen two maxima is such that they can be well distinguished), as it can be seen in Fig. 2(a), for a propagation up to $t = 10$. This may be the case when the detector is allocated relatively close to the diffractive object, so that the system has not had time enough to reach the Fraunhofer regime, where the diffraction pattern becomes stationary (its general profile does not depend on time). In such a case, we can ask ourselves questions like which parts of the diffracted beam contribute to some particular diffraction peak, or what is the contribution of a particular slit to the final intensity collected (or, equivalently, to one particular diffraction feature).

Consider the principal maxima associated with the diffraction orders $n = 0$ and $n = +1$ in Fig. 2(a). We define $\Sigma_0 = \{x_0^-, x_0^+\}$ and $\Sigma_{+1} = \{x_{+1}^-, x_{+1}^+\}$ as the regions bound by the adjacent minima to each one of these maxima, respectively, at $t = 10$ [see color shadowed regions in Fig. 2(a)]. The restricted probabilities associated with these two regions give us the value of the corresponding peak-area intensities. However, unlike the tunneling problem, the calculation of the time-evolution of these probabilities from a standard quantum point of view is here a subtler issue, for there is not a specific space region that can be uniquely defined at any time. Only once

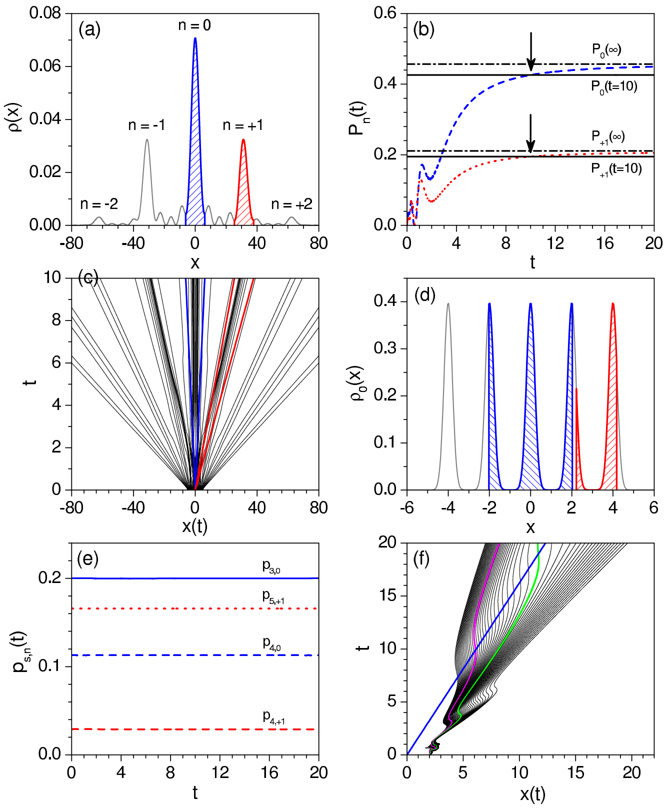

FIG. 2: (a) Interference pattern obtained from the superposition of five Gaussian wave packets at $t = 10$. Principal maxima are labeled according to their diffraction order n and the color shadowed regions denote for which the peak-area intensities are computed. (b) Peak-area intensities associated with the diffraction orders $n = 0$ (blue line) and $n = +1$ (red line). The peak-area intensities directly computed from the initial state and using the separatrix trajectories at $t = 10$ are displayed with black solid line in both cases. Black dashed lines indicate the asymptotic value of the peak-area intensities. (c) Set of quantum trajectories leaving each slit. The straight color lines delimit the tubes of probability considered to compute the peak-area intensities of the corresponding colors in panel (b). (d) Separation of the two sections in the initial probability density according to the separatrix trajectories at $t = 10$. The blue shadowed section refer to $n = 0$, while the red one to $n = +1$. (e) Contributions from slits 3, 4 and 5 [see panel (d)] to the different diffraction orders along time. (f) Set of quantum trajectories around the separatrix trajectory at $t = 10$ (purple thicker line). The right-edge boundary of the $n = 0$ probability tube is denoted with the straight blue thicker line, while a separatrix trajectory at a later time ($t \sim 20$) is denoted with green thicker line.

the maxima can be resolved (i.e., we observed a minimum between two adjacent maxima), we can consider a boundary, but not earlier, when the diffraction pattern is still in the Fresnel regime and there is no clue on which part of the pattern can be associated with a particular feature in the far field or Fraunhofer regime. Thus, the only thing we can do is to define a series of angular sectors or *probability tubes*, which start at the center of the grating and prolong (in time, because this is a one-dimensional problem) up to the position of each adjacent, vanishing minimum of a given diffraction (principal) intensity peak. That is, if such adjacent minima appear respectively at positions $\bar{x}_n^\pm$ at a time $\bar{t}$ for the maximum of order n, the time-evolution of the boundaries of the corresponding tube will be given by $x_n^\pm(t) = (\bar{x}_n^\pm/\bar{t})t$, i.e., at t the peak-intensity will be computed between $x_n^-(t)$ and $x_n^+(t)$. Note that this hypothesis is based on assuming the wave function is already well inside the Fraunhofer regime, where the minima are well defined (i.e., they are zero) and therefore the probability inside the tubes will remain constant because has already reached the stationarity (the relative shape does not change with time; time-dependent scattering approaches are based precisely on this idea [1]). This asymptotic trend can be observed in Fig. 2(b), where the peak-area intensities for the diffraction orders $n = 0$ (blue dashed line) and $n = +1$ (red dotted line) are plotted against time. As it can be seen, these quantities increase with time until they start to approach an asymptotic value, denoted by the black dashed lines. These lines denote the peak-area intensities obtained when the minima are zero and, in virtue of the non-crossing property of quantum fluxes [11], no transfer of probability is possible between adjacent maxima. In particular, at $t = 20$ the deviations with respect to the asymptotic values are about 1.72% for $n = 0$ and 1.68% for $n = +1$, which are essentially negligible.

As in the case of tunneling, if we now consider the trajectories that reach the minima adjacent to the peaks $n = 0$ and $n = +1$, we can unambiguously delimit the regions $\Sigma_0^{\rm B}$ and $\Sigma_{+1}^{\rm B}$ (the subscript "B" denotes the Bohmian simulation) that allow us to compute from the beginning the corresponding restricted probabilities. In Fig. 2(c) we observe a set of trajectories illustrating the dynamics of the diffraction process; to compare with, the thicker blue and red boundaries of the tubes binding Σ_0 and Σ_{+1}, respectively, have also been displayed. By following backwards the separatrix boundaries for $\Sigma_0^{\rm B}$ and $\Sigma_{+1}^{\rm B}$, we find the initial positions that allow us to know which portions of the initial wave function will contribute to each one of the two features considered, as shown in Fig. 2(d). In this figure we note that the central maximum is formed by the accumulation of particles that left the central slit and almost a half of the two neighboring slits. On the other hand, the maximum $n = +1$ is built up by a small portion of particles leaving the slit centered at $x = 2$ and most of those coming from the slit centered at $x = 4$. The contributions arising from each slit and each particular region of each slit remain constant along time, as shown in Fig. 2(e). Again, this is due to the non-crossing property, which avoids trajectories inside a certain tube of probability to abandon it or to allow others from outside to enter in it, thus keeping the number of them constant along time. Taking this into account, we find in Fig. 2(b) that the restricted probabilities inside the boundary trajectories displayed in Fig. 2(c) remain constant along time and, at $t = 10$, they correspond exactly with those that one would expect from the peak-area calculations (blue and red curves); the crossing between the standard and the Bohmian calculations is indicated by the downwards pointing arrows. As it can also be noted, beyond $t = 10$ these contributions are smaller than the peak-area ones, which is due to the fact that we do not have a clear distinction in terms of trajectory conditions between those trajectories that will go to the central maxima and those remaining in the adjacent secondary maxima.

As it can be seen in Fig. 2(f), which is an enlargement of panel (c), as time proceeds there are still trajectories getting into the sector associated with the maximum $n = 0$. In this panel we observe how the right-side separatrix trajectory for $t \sim 20$ (green thicker line) appears a bit further away than that for $t = 10$ (purple thicker line). Although the difference between the initial condition x_0 for these two trajectories is only about 0.030 (i.e., it is negligible in practice), as time proceeds the difference is becomes rather significant. This implies that all the trajectories between the purple and the green ones at $t = 10$ will not be considered in the calculation of $\mathcal{P}$, but only gradually at subsequent times. Of course, if we compute $\mathcal{P}$ taking into account the purple line all the way (until $t = 20$), all those trajectories between it and the boundary of the probability tube [blue thicker line in Fig. 2(f)] will not be taken into account and, therefore, the value of $\mathcal{P}$ will be slightly lower than the asymptotic value $\mathcal{P}_n(\infty)$. For example, here we find that $\mathcal{P}_0$ and $\mathcal{P}_{+1}$ are about 6.92% and 6.70% lower than the corresponding asymptotic values, which means that a 6.92% and an 6.70% of trajectories are still lacking in the calculation of the corresponding peak areas.

IV. CONCLUSIONS

Here we have presented a method that allows us to relate unambiguously final probabilities with different sections of the initial state, which is closely connected to the standard methods that can be found in statistical classical mechanics, e.g., in atmospheric modeling [19, 20]. The possibility of such a connection arises from the combination of the divergence or Gauss-Ostrogradsky theorem with Bohmian mechanics, which allows us to go a step beyond the standard formulation of quantum mechanics and devise new tools to study and to understand the physics underlying of quantum systems. In particular, even if not observable from a experimental point of view, the fact that one can properly define (in terms of separatrix trajectories) regions which are uniquely transported throughout configuration space without loss or gain of quantum flux results of much interest to study the dynamical role of quantum phase in time-resolved experiments. Note that this methodological prescription allows to monitor the detailed evolution of a set of particular initial conditions and, therefore, to determine the final outcome (probability) directly from the initial state. Actually, even if one does not know where such a particular set or part of the initial wave function will evolve, it is sure that the probability confined within its boundaries (separatrix trajectories) will not be mixed up with contributions from other parts of the same initial wave function. Within the standard scenario, however, there is no certainty about this and, therefore, one has to appeal to rather arbitrary methods to determine final restricted probabilities.

The approach posed here was aimed at computing probabilities without any need for solving the full dynamics of the process, but only with some knowledge provided by the quantum trajectories. In the literature it is also possible to find methods that operate the other way around, i.e., from probability densities they try to infer the corresponding quantum trajectories without solving the associated equations of motion. This is the case, for example, of the Bohmian Monte Carlo sampling method [21], based on the idea of quantile motion [22], or the kinematic approach [23], based on the Voronoi's tessellations method [24].

Acknowledgements Support from the Ministerio de Ciencia e Innovación (Spain) under Projects FIS2010-18132 and FIS2010-22082, as well as from the COST Action MP1006 (*Fundamental Problems in Quantum Physics*) is acknowledged. A. S. Sanz also thanks the Ministerio de Ciencia e Innovación for a "Ramón y Cajal" Research Grant.

---

[1] L. I. Schiff, *Quantum Mechanics*, 3rd ed. (McGraw-Hill, Singapore, 1968).
[2] D. J. Tannor, *Introduction to Quantum Mechanics: A Time-Dependent Perspective* (University Science Books, Sausalito, CA, 2006).
[3] D. Bohm, Phys. Rev. **85**, 166, 180 (1952).
[4] P. R. Holland, *The Quantum Theory of Motion* (Cambridge University Press, Cambridge, 1993).
[5] A. S. Sanz and S. Miret-Artés, J. Chem. Phys. **122**, 014702 (2005).
[6] A. S. Sanz, X. Giménez, J. M. Bofill, and S. Miret-Artés, Chem. Phys. Lett. **478**, 89 (2009); Chem. Phys. Lett. (Erratum) **488**, 235 (2010).
[7] A. S. Sanz, D. López-Durán, and T. Gómez-Lezana, Chem. Phys. (at press, 2011); doi:10.1016/j.chemphys.2011.07.017.
[8] A. D. Cronin, J. Schmiedmayer, and D. E. Pritchard, Rev. Mod. Phys. **81**, 1051 (2009).
[9] M. Shapiro and P. Brumer, *Principles of the Quantum Control of Molecular Processes* (Wiley, New York, 2003).
[10] H. Goldstein, C. Poole, and J. Safko, *Classical Mechanics*, 3rd ed. (Addison Wesley, New York, 2001).

[11] A. S. Sanz and S. Miret-Artés, J. Phys. A: Math. Theor. **41**, 435303(1 (2008).

[12] A. S. Sanz, F. Borondo, and S. Miret-Artés, Phys. Rev. B **61**, 7743 (2000).

[13] A. S. Sanz and S. Miret-Artés, J. Phys. A: Math. Theor. **44**, 485301(1 (2011).

[14] P. Brumer and J. Gong, Phys. Rev. A **73**, 052109 (2006).

[15] M. C. Gutzwiller, *Chaos in Classical and Quantum Mechanics* (Springer-Verlag, New York, 1990).

[16] A. S. Sanz and S. Miret-Artés, Phys. Rep. **451**, 37 (2007).

[17] R. L. Liboff, *Introductory Quantum Mechanics* (Addison-Wesley, Reading, MA, 1980).

[18] A. S. Sanz, F. Borondo, and S. Miret-Artés, J. Phys.: Condens. Matter **14**, 6109 (2002).

[19] J. Egger, Am. Meteor. Soc. **124**, 1955 (1996).

[20] M. Sommer and S. Reich, Am. Meteor. Soc. **138**, 4229 (2010).

[21] T. M. Coffey, R. E. Wyatt, and W. C. Schieve, J. Phys. A: Math. Theor. **41**, 335304 (2008).

[22] S. Brandt, H. Dahmen, E. Gjonaj, and T. Stroh, Phys. Lett. A **249**, 265 (1998).

[23] T. M. Coffey, R. E. Wyatt, and W. C. Schieve, J. Phys. A: Math. Theor. **43**, 335301 (2010).

[24] C. Fonseca-Guerra, J.-W. Handgraaf, E. J. Baerends, and F. M. Bickelhaupt, J. Comput. Chem. **25**, 189 (2004).